Fluid Phases of Highly Asymmetric Molecules: Plate-Shaped Molecules

L. K. Runnels [a] & Carolyn Colvin [a]

[a] Department of Chemistry, Louisiana State University, Baton Rouge, Louisiana, USA
Version of record first published: 21 Mar 2007.

PLEASE SCROLL DOWN FOR ARTICLE

Fluid Phases of Highly Asymmetric Molecules: Plate-Shaped Molecules†‡

L. K. RUNNELS and CAROLYN COLVIN

Department of Chemistry
Louisiana State University
Baton Rouge, Louisiana, USA

Abstract—We develop the theory of a fluid of thin plate-shaped molecules in parallel to existing theory of thin rod-shaped molecules. The molecular interactions (due to the hard core) are accounted for by a graphical expansion including 285 diagrams (through the seventh-order virial coefficients). Our simplified model envisions square tile-like molecules of vanishing thickness and only three allowed orientations. It is shown that the only irreducible diagrams of importance for this model are those for which the vertices may be colored with three (or two) colors without coloring adjacent vertices the same color. Padé analysis of the series generates a fairly stable sequence of predictions of a first-order phase transition between an isotropic low density phase and an anisotropic (but axially symmetric) higher density phase. Thermodynamic parameters characterizing the transition are remarkably similar to those characterizing the corresponding transition of a thin rod model—a similarity with some experimental reinforcement.

Introduction

There is currently a great deal of interest in the study of liquid crystals, from various points of view. Experimentally it is known that mesomorphic (liquid-crystal-forming) compounds are composed of rod-shaped, semirigid molecules.[1] And many theoretical treatments, beginning with that of Onsager,[2] have implicated high molecular asymmetry as the origin of a fluid–fluid transition.[3-8]

Strictly speaking, Onsager's analysis[2] dealt with solutions of highly asymmetric molecules in a structureless solvent. Hence the virial expansion he outlined was a series development of the osmotic

pressure of such solutions; he obtained the first nonideal term for rigid molecules of cylindrical shape. A limiting case, height much greater than diameter (" neddles "), was discussed in connection with aqueous solutions of tobacco mosaic virus—which solutions exhibit phase separation at remarkably low concentrations of tobacco virus (2% by volume). [9]

It was also pointed out that Langmuir's experiments [9] had revealed a similar phase separation, at similar concentrations, for sols of platelike particles (bentonite, iron oxide). Onsager's treatment of this limit (" pancakes "), together with Isihara's analysis of the corresponding ellipsoids, [3] suggested that theory *might* substantiate a macroscopic similarity between systems of needles and pancakes.

The whole comparison was clouded, however, by the fact that the *second* nonideal term (involving the third virial coefficient) differed greatly for the two. In fact, the third virial coefficient is vanishingly small in the needle limit, but of order one (with appropriate density units) in the pancake limit.

Zwanzig [4] patented a modification of Onsager's model which permitted the calculation of many more terms in the virial expansion of the hard rod system (now described as a " gas " rather than solution). The cylindrical needles became rectangular parallelepipeds which, moreover, could point in only three mutually perpendicular directions.

The hard rod transition signaled by the second virial coefficient treatment, is now rather completely documented as a first-order phase transformation from an isotropic (randomly oriented) phase to an anisotropic phase having axial symmetry. We present here the corresponding treatment of the related model of systems of platelike molecules. To obtain the simplicity necessary for calculation of several terms of the virial series, we also adopt here a parallelepiped model restricted in orientation to three perpendicular directions. (See Fig. 1.)

Method

In the general case, the thermodynamic properties would depend on the ratio d/l. To avoid this extra variable, the obvious model value
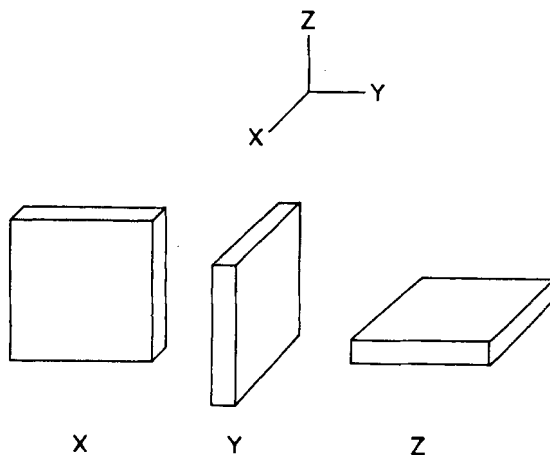
Figure 1. The model. The molecules are represented by rectangular parallelepipeds, with thickness d much less than the edge length l. Translational coordinates are continuous but orientations are limited to the three discrete perpendicular orientations shown.

is $d/l = 0$. Furthermore, setting $d = 0$ will result in additional integral simplifications, but we must be concerned with how the limit $d \to 0$ is to be taken. In our earlier treatment of rod-shaped molecules[7] the correct limiting prescription was obtained thermodynamically by showing that the ideal gas entropy of the hard rod gas contained the shape-dependent term $R \log (l^2 d)$; this arose from the moments, of inertia of the molecule. Consequently in that case the limit $d \to 0$ had to be approached with $l^2 d$ held constant.[4] It has been somewhat awkward that the hard rod molecules were thus required to be of infinite length. For the present problem, however, the ideal gas rotational entropy contains, in addition to molecular mass m and fundamental constants, the term $R \log(l^3)$. This again arises from the moments of inertia, assuming $l \gg d$. Hence, the limit $d \to 0$ should be achieved while holding l constant *and finite*. We shall take the constant to be one and employ dimensionless density units. Equivalently, the density could be regarded as having dimensions (molecules/(volume of l^3)).

We use the same general approach as before.[7] The gas is regarded as a three component system—the components being identified by the three possible orientations. The Helmholtz free energy A is calculated as a function of the three mole fractions X_i, and then

minimized with respect to variations in them. The excess free energy A_e, due to the molecular interactions, is defined by

$$A/NkT = \log \Lambda^3 - 1 + \log \rho + \sum_{i=1}^{3} X_i \log X_i + A_e/NkT, \qquad (1)$$

where $\Lambda = (h^2/2\pi mkT)^{1/2}$, A is the total free energy, ρ is the total density, and the rest of the symbols have their usual meaning. A_e is calculated by the expansion

$$A_e/NkT = -\sum_{\mathbf{n}} \mathbf{X}^{\mathbf{n}} B_{\mathbf{n}} \rho^{n-1}, \qquad (2)$$

where $\mathbf{X} = (X_1, X_2, X_3)$, $\mathbf{n} = (n_1, n_2, n_3)$ with n_i = nonnegative integer and $n = \sum n_i$, and $\mathbf{X}^{\mathbf{n}} = X_1^{n_1} X_2^{n_2} X_3^{n_3}$.

As usual, we use a graphical expansion of $B_{\mathbf{n}}$, whereby

$$B_{\mathbf{n}} = (V \prod n_i!)^{-1} \sum_{\alpha} S_{\mathbf{n}, \alpha} \qquad (3)$$

where α is a new suffix to label the irreducible (multiply connected) graphs $G_{\mathbf{n}, \alpha}$ with n_1 distinguishable vertices of color (orientation) 1, n_2 of color 2 and n_3 of color 3. The graph $G_{\mathbf{n}, \alpha}$ stands for a function of the $3n$ variables locating the centers of the n oriented molecules, and $S_{\mathbf{n}, \alpha}$ is the integral of this function over all space. The Mayer integrand $G_{\mathbf{n}, \alpha}$ vanishes for any configuration which does not produce overlap of all pairs of molecules (vertices) joined by lines of the graph. Otherwise the integrand has value $(-1)L$, where L is the number of lines in the graph. In actual practice the summation in Eq. (3) is over the various multiply connected graphs with unlabelled vertices of three colors—since the labeling does not affect the value of the integral. We must, however, multiply each graph's integral by its *degeneracy*: the number of distinguishable labeled, colored graphs which become identical if the labels are removed (but the colors retained).

There is, in the general case, one term in Eq. (3) for each distinguishable way of assigning three colors to the vertices of the star graphs that occur in the virial expansion of a one component gas of symmetric molecules.[10] Many of these terms, however, do not contribute to Eq. (3) in the limit $d \to 0$. For suppose two adjacent vertices (i.e., two vertices joined by a line) both have the same color. This requires the intersection of two parallel molecules, which occurs only in a " covolume " of order $l^2 d$; two perpendicular molecules,

on the other hand, intersect in a covolume of order l^3. In the limit $d \to 0$, $l = 1$, the difference is three dimensional measure versus two dimensional measure. Hence we include only those graphs which may be colored with three vertex colors (or two) without matching of adjacent vertices. There are several ways some graphs may be tricolored, while in other cases there is only one, or none. (See Fig. 2 and Table 1.) It should be recalled that the rigid rod limit involved even fewer of the irreducible graphs—only those which could be bicolored.[4] (i.e., there are only two colors (orientations), which alternate.) Thus all of the graphs which contribute to the virial expansion of the hard rod gas contribute to that of the hard plate gas, plus many more.
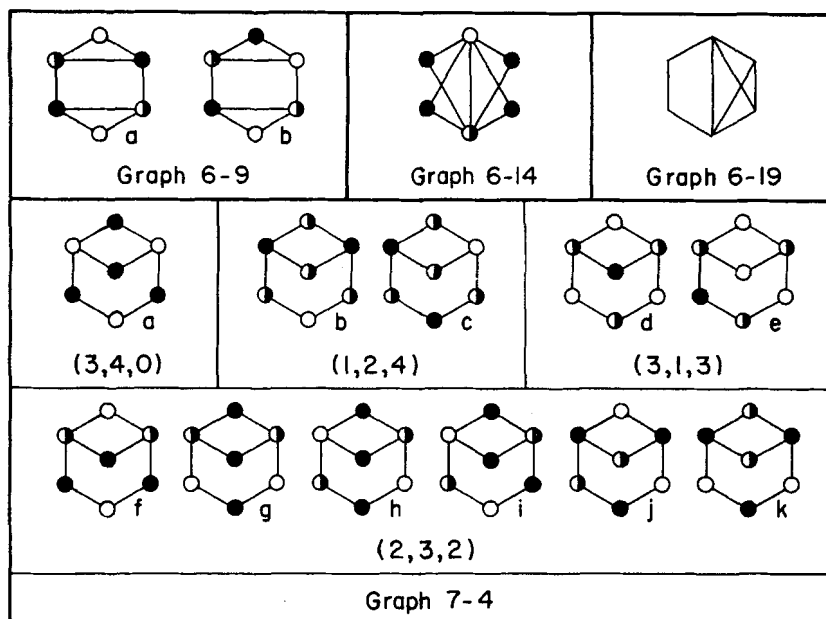
Figure 2. Examples of graph colorings. Graph 6–9 has two fundamentally different tricolorings, a and b, each employing 2 of each color. We use an open circle to denote an x-oriented molecule, a filled circle to denote a y-oriented molecule and a half-filled circle for a z-oriented molecule. The integers shown for each graph in Table 1 are the degeneracies (see Appendix) and the decimal figures are the integrals of these example graphs. Graph 6–14 allows only one tricoloring (apart from isomorphic colorings resulting from color permutations). It would require at least four colors for the vertices of graph 6–19, so it makes no contribution to the virial expansion. Graph 7–4 has a total of 11 distinct tricolorings (including the bicoloring a).

TABLE 1 Examples of Integrals and Degeneracies†

Graph	Integral	Degeneracy
6–9a	0.6815	12
6–9b	0.5602	24
6–14	− 0.4000	1
7–4a	3.9277	36
7–4b	3.1065‡	12
7–4c	2.3689	24
7–4d	3.1624	36
7–4e	3.1065‡	36
7–4f	2.5809	24
7–4g	2.7484	12
7–4h	1.9715‡	12
7–4i	1.9715‡	24
7–4j	2.6437	24
7–4k	3.3459	12

† See Fig. 2.

‡ The " accidental degeneracy " evidenced by colorings b and e and colorings h and i are a consequence of the form of the interaction (i.e., the molecular shape and orientations) assumed in the model.

In fact, with the natural density units, the contributions of the bicolored graphs are identical in the two cases *and* obtainable from the one-dimensional integrals tabulated by Hoover and DeRocco.[10] The complete integral $S_{n,\alpha}$ is a product of three factors—one arising from integrations over $x_1, x_2, x_3, ...$, one from integrations over $y_1, y_2, y_3, ...$, and a third from the z-coordinates. In the hard rod case each of these three factors is essentially the same as *the* integral for a one-dimensional hard " sphere " model of appropriate diameter. The appropriate diameter is $(l+d)/2$ in two cases and d in the third. The only difference for plate-shaped molecules is that the appropriate diameters are $(l+d)/2$ twice and l for the third direction, but the integrals still may be obtained from the work on the one-dimensional hard sphere model.

Such is not the case for the tricolored graphs, in which plates of all three orientations occur. It is still true that the total integral factors into three integrals, one for integrations along each of the three coordinate directions. But the three factors are not integrals from a one-dimensional model, since there is no single equivalent

one-dimensional length which will generate the correct integrals. This is discussed further in the Appendix, where the integration technique is presented.

In minimizing the free energy with respect to variations in the three mole fractions X_i we have not forced axial symmetry by requiring two to be equal. Instead, as in our earlier study of the hard rod case, we allow any variation subject to the single restraint $X_1 + X_2 + X_3 = 1$. There are thus two independent variables; we have used an iterative, two-dimension version of the Newton–Raphson method to locate the extrema.

We have also (hopefully) improved our estimate of the excess free energy by replacing the truncated virial series Eq. (2) by its $[m, k]$ Padé approximant,[11] *before* minimizing with respect to the mole fractions. If the highest power of ρ in Eq (2) is the Kth, we take $m = k = K/2$ if K is even or $k = m + 1 = (K + 1)/2$ if K is odd. It was found with the hard rod problem that this Padé analysis improved the convergence of the transition parameters. Preliminary study of the present problem using only the truncated series, Eq. (2), produced results so erratic and peculiar that they were of little use.

Our procedure, once the virial coefficients have been determined, then consists of the following steps: (1) for fixed density ρ, determine the minimum (with respect to mole fractions X_i) of the Padé-approximant-modified free energy; (2) calculate thermodynamic properties such as p/kT and μ/kT at the equilibrium mole fractions (i.e., at the minimum); (3) repeat steps (1) and (2) for a series of densities; (4) in the event of a " van der Waals loop ", infer a phase transition along a tie line determined by the simultaneous (graphical) solution of $(p/kT)_{p_1} = (p/kT)_{p_2}$ and $(\mu/kT)_{p_1} = (\mu/kT)_{p_2}$. The same series of steps was initially executed without replacing the truncated series for the excess free energy by its Padé approximant.

Results

In Table 2 we show explicitly the contributions to Eq. (3) of all diagrams of five or fewer points. Table 3 shows the number of contributing diagrams of seven or fewer points and Table 4 summarizes all of the calculations in the form of the virial coefficients B_n.

Direct use of the truncated series, Eq. (2), provides very little

TABLE 2   Values of Diagrams of Five Points or Fewer

Graph No.[†]	Colors	Degeneracy	I_x	I_y	I_z	$S_{n,\alpha}$
2–1	xy	1	2	2	4	− 2.0000
3–1	xyz	1	8	8	8	− 1.0000
4–1	x^2y^2	1	32	32	256	2.3704
	xy^2z	1	80	32	80	1.8518
4–2	xy^2z	1	48	32	48	− 0.6667
4–3‡						
5–1	x^2yz^2	4	352	1088	352	− 2.3808
5–2	x^2yz^2	8	352	640	256	1.0185
	x^2yz^2	4	256	1088	256	1.2593
5–3	x^2y^3	1	192	192	3072	2.0000
	xy^3z	1	576	192	576	1.1250
	x^2yz	2	448	1088	192	1.6528
5–4	xy^3z	1	384	192	384	− 0.5000
5–5	x^2yz^2	4	256	384	256	− 0.4444
5–6	x^2yz^2	4	256	640	192	− 0.5556
5–7‡						
5–8	x^2yz^2	1	192	384	192	0.2500
5–9‡						
5–10‡						

† As tabulated in Ref. (10).   For graphs of five points or fewer, the colors used uniquely define the graph coloring except for graph 5–2; the colorings are defined uniquely by the degeneracies for that graph.

‡ No tricolored graphs.

TABLE 3   Numbers of Irreducible Graphs (Stars)

Number of points, n	Stars of n points	Bicolored stars of n points	Tricolored stars of n points†
2	1	1	1
3	1	0	1
4	3	1	2
5	10	1	7
6	56	5	35
7	468	8	239

† Includes every bicolored star, since a bicolored star may always be tricolored.

information, other than the qualitative indication that *something* happens at densities greater than about 1.5.   At lower densities an isotropic fluid $(X_1 = X_2 = X_3 = \frac{1}{3})$ is the only extremum (minimum) of the free energy, as we would expect.   The anticipated transition

to an orientationally ordered fluid at higher densities cannot really be proclaimed on the basis of the truncated series work. It is true that (axially symmetric) minima do occur, but there is erratic change as the order of the approximation changes. And the " stable " phase (i.e., that associated with the minimum in A) is often quite unphysical. Besides occurring with " two-dimensional ordering " (such as $X_1 = X_2 = 0.45$, $X_3 = 0.1$, for example), the high density phases often have negative compressibility, and even negative pressure at high enough densities.

This wild behavior is not really so surprising if Table 4 is taken into account The coefficients B_n are not decreasing regularly as $n = n_1 + n_2 + n_3$ increases. Under such circumstances reliable estimates of the excess free energy at higher densities is hardly to be expected. It may be seen that the situation is considerably worse than for the hard rod case (coefficients with n of the form $(m, l, 0)$).

TABLE 4   Free Energy Coefficients B_n

$n = (j, k, l)$	B_n	
	Rational	Decimal
(1, 1, 0)	-2	-2.000
(1, 1, 1)	-1	-1.000
(1, 1, 2)	16/27	0.5926
(2, 2, 0)	16/27	0.5926
(2, 2, 1)	695/864	0.8044
(1, 1, 3)	5/48	0.1042
(2, 3, 0)	1/6	0.1667
(2, 2, 2)	51077/108000	0.4729
(1, 2, 3)	$-35839/216000$	-0.1659
(1, 1, 4)	2/125	0.0160
(3, 3, 0)	$-1352/6750$	-0.2003
(2, 4, 0)	16/375	0.0427
(2, 3, 2)	$-918787/2332800$	-0.3939
(3, 1, 3)	$-17517911/23328000$	-0.7509
(1, 2, 4)	$-62137/486000$	-0.1279
(3, 4, 0)	$-916/6075$	-0.1508
(1, 1, 5)	7/3240	0.0022
(2, 5, 0)	4/405	0.0099

TABLE 5   Transition Parameters†

Approximant (m, k)	p/kT	μ/kT	Isotropic Density	Mesophase Density	z‡
(1, 2)	2.22	0.75	1.21	1.72	0.91
(2, 2)§	...	...	...	...	...
(2, 3)	2.67	0.96	1.76	2.24	0.91
(3, 3)	2.58	0.92	1.60	2.02	0.88

† The corresponding estimates for the hard rod case, from the (3, 4) approximant, are $p/kT = 2.51$, $\mu/kT = 0.89$, densities $= 1.45$ and 1.93, and $z = 0.88$. All chemical potentials μ/kT in Ref. (7) are erroneously high by a constant term $\ln 3 = 1.0986$.

‡ The unique mole fraction in the mesophase. The other two are each $(1 - z)/2$.

§ " Two-dimensional ordering." That is, the unique mole fraction is less than 0.5. Furthermore, this mesophase has negative compressibility.

The situation seems to be improved considerably by Padé analysis. As shown in Table 5, a reasonably stable sequence of transition parameters is provided by the (m, k) Padé approximants. While these parameters are not determined to high accuracy, the existence of the transition and its general characteristics seem to be indicated fairly clearly. All extrema are axially symmetric—i.e., there are at least two equal mole fractions. Our best estimate of the equation state is shown in Fig. 3.

The comparisons between the transition parameters and those of the hard rod case are intriguingly close. In the simplest possible treatment of the two cases, i.e., the second virial approximation (0, 1), the transition parameters are identical. This is true because both expansions would involve only B_{110} (and B_{101} and B_{011}). The equations of state cannot be identical, however, since the third derivatives (of p/kT with respect to ρ) differ at $\rho = 0$. Nonetheless, it does appear that our more extended treatment preserves the macroscopic similarity of the two systems indicated earlier by experiment[9] and initial analyses. [2,3]

Appendix.   The Integrals and Degeneracies

As discussed in the text we need to determine those star graphs (as tabulated by Hoover and DeRocco[10]) whose vertices may be colored
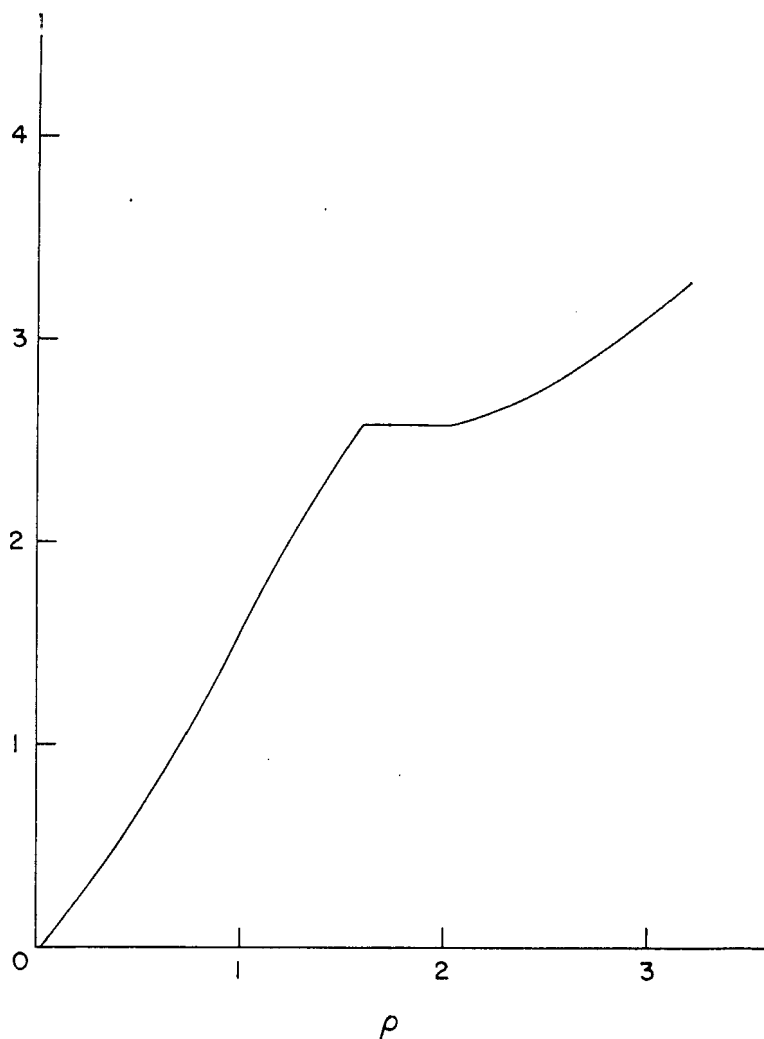
Figure 3. Equation of state in the limit $d \to 0$. The ordinate is actually Pl^3/kT and the abscissa is Nl^3/V. We have set $l = 1$. This curve is the one calculated from the (3, 3) approximant.

with three or two colors without matching colors of adjacent vertices. The bicolored graphs have previously been determined and evaluated, so we focus our attention on the tricolored graphs.

It is easy to characterize a graph which may be bicolored:[12] it contains no odd cycles. The corresponding characterization of tricolored graphs has not been discovered, so we have determined empirically (with a computer program) which of the stars of seven

or fewer points may be tricolored (see Table 3).   At least a subset of the nontricolored graphs may be characterized by the rule that such a graph contains a vertex which is adjacent to every vertex of an odd cycle.   The simplest is the complete graph of four points (a tetrahedron).   The next simplest is a pentagonal pyramid (or the Chrysler symbol).   It is easy to see that these graphs cannot be tricolored, but whether or not all nontricolored graphs may be so characterized is not known.   Empirically the rule is adequate for irreducible graphs of seven points or fewer.

The same computer program also determined the degeneracies of the permissible colorings.   In the language of combinatorial analysis, our graph colorings correspond to ordered partitions (or compositions) of three parts.   For a coloring n with no repeated parts, such as (1, 2, 4) of graph 7–4, the degeneracy is given by

$$\frac{n_1!\ n_2!\ n_3!}{\sigma},$$

where σ is the number of color-preserving permutations of the vertices which are symmetry operations of the graph.   Of course we determine only the contributions to the virial coefficient for $n = (1, 2, 4)$, since, for example, the coefficient for (2, 4, 1) will clearly have the same value.

Another factor must be taken into account when the coloring contains repeated parts, such as (3, 1, 3) of graph 7–14.   If interchange of the equally numerous colors is not a symmetry operation of the colored graph, then the graph with the interchanged colors must be included also.   But since the integrals would clearly be equal, it suffices simply to let the interchange contribute to the degeneracy of one representative form.   Thus graph coloring 7–4d would have a degeneracy of only 18 if it did not also represent the graph with open and half-filled circles interchanged.   Similarly the degeneracies of each (2, 2, 2) coloring of graph 6–9 include a factor of 3 to provide for nonequivalent graphs produced by color permutations.   (Half of the 6 possible permutations *are* symmetry operations.)   It should be noticed, however, that no such factor is present in graph coloring 7–4j, for interchange of open and half-filled circles does not produce a distinguishable graph coloring.

Turning now to the actual evaluation of the integrals, we have

used basically the integration scheme previously employed in connection with the hard rod gas. [7] There are, however, some modifications required by the presence of three molecular orientations. Since each Mayer f-factor represented by the lines in the diagrams may be written as the product $f = f_x f_y f_z (= 0$ or $-1)$, the entire integrand still factors into a product of three integrals, one arising from integrations along each of the three coordinate axes.

For an example we consider graph 7–4 with coloring b, numbering the vertices clockwise beginning at the top and numbering the central vertex seven. The essence of the Mayer factor for hard parallelepiped molecules is that two molecules intersect only if their projections intersect on *each* of the three coordinate axes. This is the origin of the factoring of the integral. The projections of the molecules, however, differ in the three directions. For the x-integrations we may imagine the molecules all projected onto the x-axis—whereby (in the limit $d \to 0$, $l = 1$) an x-oriented molecule becomes a point, while a y- or z-oriented molecule becomes a line of length one. To view the required intersections we may transcribe the lines of 7–4b into " long bonds " and " short bonds ", the former occurring between molecule projections which are both of length one and the latter representing the case of a line and a point. Thus short bonds emanate from vertices whose color (orientation) is the same as the coordinate axis of the current integrations. Figure 4 shows the three projection diagrams for graph coloring 7–4b. Only in a " homogeneous " case such as for the z-projection of 7–4b, where all bonds have the same length, may the integral be obtained from the one-dimensional hard rod integrals tabulated by Hoover and DeRocco. [10]

The " short bond " between molecules 3 and 4 in the x-projection means, for example, the requirement that $|x_3 - x_4| \leqslant \frac{1}{2}$. The "long bond " between molecules 1 and 2 means $|x_1 - x_2| \leqslant 1$. For convenience, however, we have doubled all lengths and later we divide the entire integral by $2^{3(n-1)}$. The integrals are also divided by the total volume V (see Eq. (3)), which is equivalent to confining one molecule (number n) to the origin and measuring the other molecular centers relative to it.

Each of the integrals represented by diagrams such as in Fig. 4 are thus related to the " volume " of a six-dimensional region
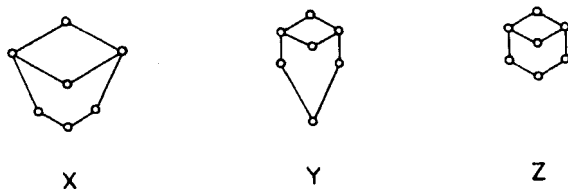
X   Y   Z

Figure 4.   Diagrams depicting the three factor integrals arising from graph coloring 7–4b of Fig. 2.   A " short bond " between two vertices indicates that the integrand vanishes unless the centers of the corresponding projected molecules are no more distant than one; the " long bond " allows the molecules to be twice as far apart.

(molecule 7 fixed) in which all required inequalities of the form $|x_3 - x_4| \leqslant 1$ and $|x_1 - x_2| \leqslant 2$ are satisfied.   This region is thus bounded by hyperplanes (with equations such as $x_3 = x_4 + 1$, etc.) and its " volume " is best determined by our procedure described earlier.[7] This scheme divides 6-space into unit 6-cubes and determines for each the content of the region enclosed by the bounding hyperplanes —these contents must necessarily be integral multiples of $(\frac{1}{5}!)$, and we denote these integers by I_x, I_y, I_z.   (See Table 2.)   The more general statement is that for a tricolored diagram of n points, one of them stationary, the integral is of the form

$$S_{n,\alpha} = \frac{I_x \cdot I_y \cdot I_z}{2^{3n-3}[(n-1)!]^3} \tag{4}$$

In the case of 7–4b, the numerator is 303 953 996 677 120.

Since we have determined all integrals as rational numbers, their summations to give the virial coefficients are also obtainable as rationals (Table 4).   It was only for the minimization of the free energy that the decimal equivalents were introduced (as double precision floating point numbers).

REFERENCES

1. Gray, G. W., *Molecular Structure and the Properties of Liquid Crystals* (Academic Press, New York, 1962).
2. Onsager, L., *Ann. N.Y. Acad. Sci.* **51**, 627 (1949).
3. Isihara, A., *J. Chem. Phys.* **19**, 1142 (1951).
4. Zwanzig, R., *J. Chem. Phys.* **39**, 1714 (1963).
5. Wulf, A. and DeRocco, A. G., in Johnson, J. F. and Porter, R. S. (Eds.), *Liquid Crystals and Ordered Fluids* (Plenum Press, New York, 1970), p. 227.

6. Cotter, M. A. and Martire, D. E., *J. Chem. Phys.* **52**, 1902, 1909 (1970).
7. Runnels, L. K. and Colvin, Carolyn, *J. Chem. Phys.*, to be published.
8. Hubbard, J. B. and Runnels, L. K., to be published.
9. Langmuir, I., *J. Chem. Phys.* **6**, 873 (1938).
10. Hoover, W. G. and DeRocco, A. G., *J. Chem. Phys.* **36**, 3141 (1962).
11. Baker, G., Jr., *Advan. Theoret. Phys.* **1**, 1 (1965).
12. Busacker, R. G. and Saaty, T. L., *Finite Graphs and Networks* (McGraw-Hill Book Company, New York, 1965), p. 86.